The Plant Cell, Vol. 27: 1670–1680, June 2015, www.plantcell.org

The Arabidopsis SWI2/SNF2 Chromatin Remodeling ATPase BRAHMA Targets Directly to *PINs* and Is Required for Root Stem Cell Niche Maintenance

Songguang Yang,[a,b,1] Chenlong Li,[c,d,1] Linmao Zhao,[a,1] Sujuan Gao,[e] Jingxia Lu,[a] Minglei Zhao,[a] Chia-Yang Chen,[b] Xuncheng Liu,[a] Ming Luo,[a] Yuhai Cui,[c] Chengwei Yang,[f] and Keqiang Wu[b,2]

[a] Key Laboratory of South China Agricultural Plant Molecular Analysis and Gene Improvement, South China Botanical Garden, Chinese Academy of Sciences, Guangzhou 510650, China
[b] Institute of Plant Biology, National Taiwan University, Taipei 106, Taiwan
[c] Southern Crop Protection and Food Research Centre, Agriculture and Agri-Food Canada, London, Ontario N5V 4T3, Canada
[d] Department of Biology, Western University, London, Ontario N6A 5B7, Canada
[e] College of Light Industry and Food Science, Zhongkai University of Agriculture and Engineering, Guangzhou 510225, China
[f] Guangdong Key Lab of Biotechnology for Plant Development, College of Life Science, South China Normal University, Guangzhou 510631, China

ORCID IDs: 0000-0002-3675-3288 (Y.C.); 0000-0002-5791-3594 (K.W.)

BRAHMA (BRM), a SWI/SNF chromatin remodeling ATPase, is essential for the transcriptional reprogramming associated with development and cell differentiation in *Arabidopsis thaliana*. In this study, we show that loss-of-function mutations in *BRM* led to defective maintenance of the root stem cell niche, decreased meristematic activity, and stunted root growth. Mutations of *BRM* affected auxin distribution by reducing local expression of several *PIN-FORMED* (*PIN*) genes in the stem cells and impaired the expression of the stem cell transcription factor genes *PLETHORA* (*PLT1*) and *PLT2*. Chromatin immunoprecipitation assays showed that BRM could directly target to the chromatin of *PIN1*, *PIN2*, *PIN3*, *PIN4*, and *PIN7*. In addition, genetic interaction assays indicate that *PLTs* acted downstream of *BRM*, and overexpression of *PLT2* partially rescued the stem cell niche defect of *brm* mutants. Taken together, these results support the idea that *BRM* acts in the PLT pathway to maintain the root stem cell niche by altering the expression of *PINs*.

INTRODUCTION

Plant roots form from a reservoir of undifferentiated cells, the root stem cells, in the root apical meristem. Within the root meristem, the quiescent center (QC), a small group of mitotically inactive cells, maintains the root stem cells. The QC generates unknown, non-cell-autonomous signals that prevent differentiation of the stem cells, through direct cell-cell contacts (van den Berg et al., 1997). This short-range signaling restrains the division of stem cells so that the stem cells do not become displaced from the growing root tip.

Two main pathways, the PLETHORA (PLT) pathway (Aida et al., 2004; Blilou et al., 2005) and the SHORT-ROOT (SHR)/SCARECROW (SCR)/RETINOBLASTOMA RELATED pathway (Helariutta et al., 2000; Nakajima et al., 2001; Sabatini et al., 2003; Wildwater et al., 2005), act to specify the stem cell niche. SHR and SCR also act upstream of the PLTs, as *shr-2* and *scr-4* mutants show decreased expression of *PLT1* and *PLT2* (Aida et al., 2004; Koizumi and Gallagher, 2013). *SHR* and *SCR*, which encode members of the plant-specific GRAS family of putative transcription factors, are required for stem cell maintenance. Genetic and molecular data indicate that *SHR* is expressed in the central stele tissue where the vasculature forms; SHR subsequently moves into the surrounding tissue layer to directly activate *SCR* expression by binding to the *SCR* promoter (Levesque et al., 2006; Cui et al., 2007). SCR forms a heterodimer with SHR to inhibit the binding of SHR at the *SCR* promoter. This feedback loop is thought to enable the rapid upregulation of *SCR* expression and limit the movement of SHR to a single cell layer adjacent to the stele.

The auxin-inducible *PLT1* and *PLT2* genes, which encode members of the AP2 class of transcription factors, are also essential for root stem cell niche maintenance (Aida et al., 2004; Galinha et al., 2007). PLTs function as dose-dependent regulators: High concentrations of PLTs maintain the QC and stem cell activity, intermediate concentrations regulate the division and differentiation of the transit-amplifying cells, and low concentrations allow differentiation to proceed (Galinha et al., 2007). Interestingly, the expression of *PLT* genes requires auxin response transcription factors and forms gradients that are thought to be a readout of an underlying auxin gradient (Aida et al., 2004; Galinha et al., 2007; Grieneisen et al., 2007). The PLT gradient is not a direct, proportionate readout of the auxin gradient. Rather, prolonged high auxin levels generate a narrow domain of *PLT* transcription, which generates a gradient of PLT

[1] These authors contributed equally to this work.
[2] Address correspondence to kewu@ntu.edu.tw.
The author responsible for distribution of materials integral to the findings presented in this article in accordance with the policy described in the Instructions for Authors (www.plantcell.org) is: Keqiang Wu (kewu@ntu.edu.tw).
www.plantcell.org/cgi/doi/10.1105/tpc.15.00091

protein through slow growth dilution and cell-to-cell movement (Mähönen et al., 2014). In addition, the gradient expression of *PLTs* is PIN dependent in controlling auxin-mediated root patterning. PIN proteins restrict *PLT* transcription in the basal embryo region to initiate root primordium formation. Conversely, the transcription of *PINs* that stabilizes the position of the stem cell niche is maintained by PLTs (Blilou et al., 2005; Grieneisen et al., 2007; Dinneny and Benfey, 2008).

The ATP-dependent SWI/SNF chromatin remodeling complexes affect gene expression by using the energy of ATP hydrolysis to alter the interactions between histones and DNA to create accessible DNA (Cairns, 2005). *SWI* and *SNF* were first identified from *Saccharomyces cerevisiae* by the examination of mating type switching (*SWI*) and sucrose nonfermenting (*SNF*) mutants (Neigeborn and Carlson, 1984; Stern et al., 1984). Biochemical analysis demonstrated that the yeast SWI/SNF complexes possess a catalytic subunit (ATPase) and 10 accessory core subunits (Cairns et al., 1994; Peterson et al., 1994) and can facilitate binding of transcription factors to nucleosomal DNA (Côté et al., 1994). Although the SWI/SNF complexes have been shown to play a central role in animal development and cell differentiation (Pedersen et al., 2001; Ohkawa et al., 2006), relatively little is known about their functions in plants. Nevertheless, genome analysis suggests that the *Arabidopsis thaliana* genome encodes more than 40 ATPases of the SNF2 family, four of which (BRM, SPLAYED [SYD], CHR12, and CHR23) belong to the SWI2/SNF2 subfamily based on phylogenetic analysis of the SNF2 ATPase catalytic domains (Knizewski et al., 2008). Several lines of evidence suggest that BRM is the ATPase of at least one of the putative SWI/SNF complexes in Arabidopsis. BRM has all the domains, including a C-terminal bromodomain that is a characteristic of ATPases of SWI/SNF complexes in yeast and *Drosophila melanogaster* (Knizewski et al., 2008).

Recent data suggest that BRM plays a crucial role in vegetative, embryonic, and reproductive plant development (Kwon et al., 2006; Jerzmanowski, 2007; Tang et al., 2008; Han et al., 2012; Wu et al., 2012; Efroni et al., 2013; Zhu et al., 2013; Vercruyssen et al., 2014). Indeed, Arabidopsis *BRM* is primarily expressed in meristems, organ primordia, and tissues with active cell division (Farrona et al., 2004). The *brm* mutant shows pleiotropic phenotypes, such as reduced plant size with short roots (Farrona et al., 2004; Hurtado et al., 2006), downward-curling leaves (Hurtado et al., 2006), hypersensitivity to abscisic acid (Han et al., 2012), and early flowering (Farrona et al., 2004, 2007). Recent work showed that the SYD and BRM ATPases interact with LEAFY and SEPALLATA3 proteins involved in controlling floral organ identity and act antagonistically with Polycomb repressors (Wu et al., 2012; Li et al., 2015). In addition, BRM associates with TCP4, ANGUSTIFOLIA3, and BREVIPEDICELLUS (BP) to regulate leaf development and inflorescence architecture (Efroni et al., 2013; Vercruyssen et al., 2014; Zhao et al., 2015).

In this study, we show that mutations of *BRM* led to defective root stem cell niche maintenance. BRM specifically bound to *PIN* loci and activated the expression of *PIN* genes. Overexpression of *PLT2* partially rescued the stem cell niche defect of *brm-3* mutants, indicating that BRM affects root stem cell niche maintenance mainly through the PLT pathway.

RESULTS

BRM Mutations Cause Stunted Root Growth and Reduced Root Meristem Size

To investigate the role of BRM in root development, we analyzed the phenotype of three *brm* mutant alleles, *brm-1*, *brm-3*, and *brm-5*. The *brm-1* and *brm-3* alleles carry T-DNA insertions in the first exon and 11th intron of *BRM* (Hurtado et al., 2006; Farrona et al., 2007), respectively; *brm-5* is an ethyl methanesulfonate mutant (Tang et al., 2008). Previous studies indicated that disruption of *BRM* causes pleiotropic defects in shoots (Farrona et al., 2004) and short roots (Hurtado et al., 2006; Wu et al., 2012). Plants carrying the null mutant allele *brm-1* are sterile, since *brm-1* flowers fail to open at maturity and cannot set seeds (Kwon et al., 2006), whereas plants carrying the weak alleles *brm-3* and *brm-5* are fertile. We also observed the short root phenotype in *brm-1*, *brm-3*, and *brm-5* mutant seedlings (Figure 1A). The primary root length of *brm-1* mutant seedlings was significantly reduced compared with the weak alleles, *brm-3* and *brm-5*, at 7 d after germination (DAG) (Figure 1A). The growth rate of the primary root was markedly reduced in *brm-1*, *brm-3*, and *brm-5* mutants as early as 2 DAG (Figure 1B). At 10 DAG, the primary root lengths of *brm-1*, *brm-3*, and *brm-5* seedlings were only ~29, 54, and 60% of the wild type (Figure 1B). Compared with the wild type, *brm-1*, *brm-3*, and *brm-5* seedlings showed significantly smaller meristem sizes at different DAG (Figure 1C). The differentiated epidermal cells of *brm-1*, *brm-3*, and *brm-5* plants at 5 DAG were significantly smaller than those of the wild type (Figure 1D).

Consistent with previous data (Jerzmanowski, 2007), more lateral roots were observed in *brm-1*, *brm-3*, and *brm-5* mutant seedlings after 10 DAG (Supplemental Figure 1), suggesting that *BRM* may also play a role in lateral root development. The expression of *CycB1;1* and *CycB1;3*, two markers for the G2/M phase of the cell cycle (Colón-Carmona et al., 1999), was reduced in *brm-3* mutants (Supplemental Figure 2), indicating that the population of dividing cells is highly reduced in these mutants. Collectively, these results indicate that the short-root phenotype of *brm* mutants results from effects on both the cell division activity of root meristems and on cell elongation.

BRM Regulates Stem Cell Niche Maintenance

The observation that *BRM* is crucial for maintaining meristem sizes in roots prompted us to investigate its possible effects on the cellular organization of the QC and surrounding stem cells. The QC cells can be easily discerned by confocal microscopy in wild type (Figure 2A), and the pattern of cells in the root tips of *brm-3* and *brm-5* roots was not disrupted (Supplemental Figure 3A). However, the pattern of cells was disrupted in *brm-1* root tips and the QC could not be identified morphologically (Figure 2A). In addition, the differentiated columella area next to columella stem cells (CSCs) in *brm-1* mutants consists of irregularly shaped cells (Figure 2A; Supplemental Figure 3A). Furthermore, the presence of starch granules, which mark differentiated columella cells, were found in the CSC area in *brm-1* roots (Figure 2B). These data indicate that the activity of CSC was decreased in

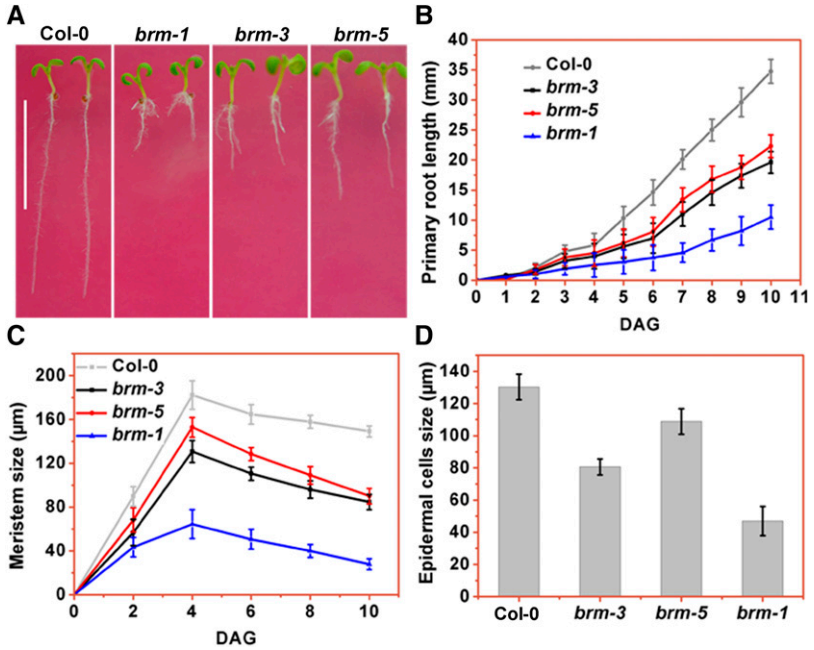

Figure 1. *BRM* Deficiency Leads to Reduced Root Meristem Size and Stunted Root Growth.

(A) Phenotypes of wild-type (Columbia-0 [Col-0]), *brm-3*, *brm-5*, and *brm-1* seedlings at 7 DAG. Bar = 1 cm.
(B) Primary root length of wild-type (Col-0), *brm-3*, *brm-5*, and *brm-1* seedlings from 0 to 10 DAG. Data shown are means ± SD (n = 30).
(C) Root meristem size of the wild-type (Col-0), *brm-3*, *brm-5*, and *brm-1* seedlings from 0 to 10 DAG. The root meristem size is expressed as the length from cortex cells in QC to the transition zone. Data shown are means ± SD (n = 25).
(D) The size of differentiated epidermis cells of the wild-type (Col-0), *brm-3*, *brm-5*, and *brm-1* seedlings at 5 DAG. Data shown are means ± SD (for the wild type, *brm-3*, and *brm-5*, n = 40; for *brm-1*, n = 20).

brm-1 roots. Similar results were also observed in the *brm-3* and *brm-5* mutants (Figure 2B). Furthermore, the 4th differentiated columella cells in *brm-3* and *brm-5* were remarkably smaller compared with those of the wild type (Supplemental Figure 3B).

To further investigate whether the disruption of the stem cell niche is associated with misspecification of the QC, we monitored the expression of three independent QC-specific markers (*QC25*, *QC46*, and *QC184*) as indicated by the β-glucuronidase (GUS) reporter in *brm* mutants. We selected the hypomorphic *brm-3* and *brm-5* alleles for further analysis because they are fertile, which facilitated testing of homozygous mutant embryos. In wild-type plants, *QC25* and *QC46* were expressed in QC cells (Figure 2C). In a large proportion of *brm-3* roots, however, *QC25* and *QC46* expression were either absent or highly reduced (Figure 2C, Table 1). Similarly, another QC marker *QC184* was also aberrantly expressed in the *brm-3* roots (Table 1). These results indicate that *BRM* is essential for proper QC identity and CSC activity.

Mutation of *BRM* Affects the Expression of *PINs* in the Root Tip

In Arabidopsis root development, auxin regulates pattern formation as well as the orientation and extent of cell division (Sabatini et al., 1999). Polar auxin transport is a major factor in organ formation, such as the initiation of lateral roots and leaf primordia (Benková et al., 2003; Friml et al., 2003; Reinhardt et al., 2003). To investigate whether the *brm-3* short root phenotype was related to auxin, we first monitored auxin accumulation using the *DR5:GFP* (green fluorescent protein) reporter (Ulmasov et al., 1997). We found that even though the expression of *DR5:GFP* in the *brm-3* root tip showed reduced expansion compared with the wild type, the expression maxima of *DR5:GFP* localized in the center of the root meristem (Figures 3A to 3B). Next, we examined the auxin efflux transporter genes, *PINs*, which play an important role in stem cell niche maintenance (Friml et al., 2003; Blilou et al., 2005). The expression levels of *PIN1* and *PIN2*, as shown by the *PIN1:GFP* and *PIN2:GFP* promoter fusion reporters (Figures 3C to 3D; Supplemental Figure 4A), were obviously reduced in the *brm-3* root tip as marked by fluorescence (Figure 3E). Meanwhile, the transcript levels of *PIN1* and *PIN2* were also reduced in the *brm-3* root tips and *brm-1* seedlings (Figure 3F; Supplemental Figure 4B). In addition, similar to the previous microarray data using 18-d-old *brm-1* seedlings (Archacki et al., 2013), the levels of *PIN3*, *PIN4*, and *PIN7* were also reduced in *brm-3* root tips (Figure 3F). Collectively, our data suggest that the short-root phenotype of *brm* was likely caused by reduced expression of the auxin transport-related genes and the concomitant alteration of local auxin distribution in the root tip.

BRM Affects *PLT1* and *PLT2* Expression

As noted above, in Arabidopsis, two main pathways are involved in root stem cell niche maintenance (Aida et al., 2004). The SHR/SCR pathway provides positional information along the radial

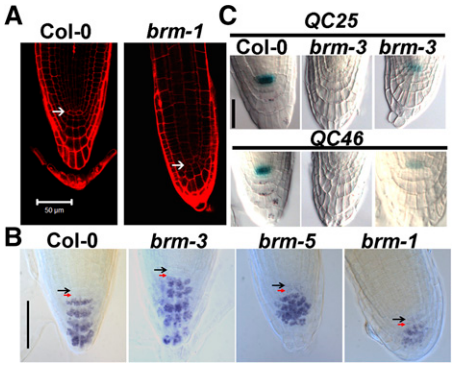

Figure 2. *BRM* Mutants Show Defective Root Stem Cell Niche Maintenance.

(A) Cellular organization of wild-type and *brm-1* root tips at 3 DAG using PI staining. The white arrow shows the QC cells. Bars = 50 μm.
(B) Lugol-stained (light blue) roots of the wild type (Col-0), *brm-3*, *brm-5*, and *brm-1* at 3 DAG. Black and red arrows indicate QC and columella initials (CSC), respectively. Bars = 50 μm.
(C) The expression *QC25* and *QC46* GUS markers in the wild type (Col-0) and *brm-3* at 3 DAG. Bars = 25 μm.

axis, whereas the PLT1/PLT2 pathway provides longitudinal information. To determine whether the disturbed stem cell niche in the *brm* mutants was caused by misregulation of these stem cell niche-defining transcription factors, we examined the expression pattern of these genes in *brm-3* at 3 DAG. We first monitored the expression of *SHR/SCR* using SHR_{pro}*:GFP*/SCR_{pro}*:GFP* in the *brm-3* mutants. The expression and localization of *SHR* (Supplemental Figure 5A) and *SCR* (Supplemental Figure 5C) were not affected in *brm-3* mutants compared with the wild type. In addition, the root lengths of *brm-3 shr-1* and *brm-3 scr-1* double mutants were shorter than those of *brm-3*, *shr-1*, and *scr-1* single mutants (Supplemental Figures 5B and 5D). Similar results were also observed in roots of plants carrying the null allele *brm-1* (Supplemental Figures 5E to 5F). These data support that *BRM* acts in parallel with the SHR/SCR pathway.

To test whether mutations of *BRM* affect the expression of *PLT* genes, we quantified the *PLT1* and *PLT2* transcripts in the roots of wild-type, *brm-3*, *brm-5*, and *brm-1* seedlings using reverse transcription-quantitative PCR (RT-qPCR) assays. The data showed that *PLT1* and *PLT2* transcripts were markedly reduced in *brm* mutants (Figure 4A; Supplemental Figure 4B). Similarly, yellow fluorescent protein (YFP) levels of the translational fusions, PLT1:YFP and PLT2:YFP, were also reduced in *brm-3* compared with the wild type (Figures 4B to 4C), suggesting that loss of *BRM* activity also affects PLT1 and PLT2 expression at the protein level. Taken together, our results reveal that the defective stem cell niche maintenance in the *brm* mutants is correlated with a dramatic misregulation of *PLT1* and *PLT2* expression.

To assess whether BRM acts in the PLT pathway, *brm-3* plants were crossed to *plt1 plt2* double mutant plants (Aida et al., 2004). The root lengths and meristem sizes of *brm-3 plt1-4 plt2-2* and *brm-1 plt1-4 plt2-2* triple mutants were similar to those of *plt1-4 plt2-2* double mutants (Figures 4D and 4E; Supplemental Figure 6), confirming that BRM acts in the PLT pathway.

We further determined whether overexpression of *PLT* genes can rescue the *brm-3* mutant phenotype. The inducible expression construct *35Spro:PLT2:GR* (Galinha et al., 2007) was introduced into *brm-3* through genetic crossing. A short-term induction (2 d) of *PLT2* expression by adding dexamethasone (DEX) did not severely affect the growth of wild-type and mutant seedlings (Figure 5A). Consistent with previous reports (Galinha et al., 2007; Kornet and Scheres, 2009), a short-term induction of *PLT2* expression by DEX led to a substantial increase of the meristem cell number in wild-type roots (Figures 5B and 5C). In the *brm-3* background, the cell number of the meristem also significantly increased after DEX induction (Figures 5B and 5C), similar to the wild type with DEX induction (Figure 5C). About 48.1% of *brm-3* seedlings (n = 56) possess meristem sizes similar to the wild type without DEX induction (Figure 5B). In addition, DEX induction substantially improved the length of columella cells in the $35S_{pro}$*:PLT2:GR/brm-3* seedlings (Figure 5B). Together, these data indicate that overexpression of *PLT2* can, at least partially, rescue the root meristem defects of *brm-3*, supporting the idea that *BRM* acts in the PLT pathway.

BRM Directly Targets to *PIN* Loci in Roots

As described above, we observed markedly reduced transcript levels of *PINs* and *PLTs* in *brm-3* roots. Next, we investigated whether the effect of BRM on the mRNA accumulation of *PINs* and *PLTs* is direct or indirect. To test for binding of BRM to *PIN* and *PLT* loci, a GFP-tagged BRM (BRM_{pro}*:BRM:GFP*) (Smaczniak et al., 2012; Li et al., 2015) that fully rescued the root meristem defects of the *brm-1* null mutant (Supplemental Figure 7) was

Table 1. The Expression of QC Markers in the Wild Type and *brm-3* Mutants

QC Markers	No Expression		Reduced Expression		Expanded Expression		Normal Expression		Total Numbers	
	Wild Type	*brm-3*	Wild Type	*brm-3*	Wild Type	*brm-3*	Wild Type	*brm-3*	Wild Type	*brm-3*
QC25	8.3%	24.3%[a]	16.4%	32.4%[a]	6.8%	8.2%	68.5%	35.1%	67	85
QC46	10.5%	31.2%[a]	10.3%	30.6%[a]	11.3%	13.7%	67.9%	24.5%	52	62
QC184	11.8%	38.1%[a]	13.2%	29.4%[a]	9.6%	10.8%	65.4%	21.7%	58	54

The GUS staining areas were measured using Digimizer image analysis software (http://www.digimizer.com). The staining areas between 50 and 90 μm^2 were defined as "normal expression" (Supplemental Figure 10), <50 μm^2 as "reduced expression," and more than 90 μm^2 as "expanded expression."
[a]One-way ANOVA (Student's t test) analysis was performed, and statistically significant differences ($P < 0.05$) are indicated.

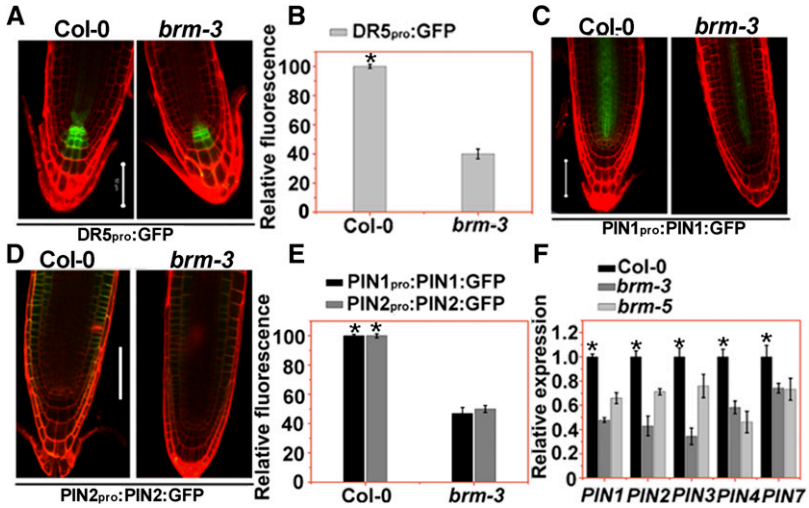

Figure 3. Mutations of *BRM* Affects the Contents of Auxin and the Expression of *PIN* Genes

(A) Expression pattern of the $DR5_{pro}$*:GFP* reporters in the wild type (Col-0) and *brm-3* at 3 DAG. Bars = 50 μm.
(B) Quantification of $DR5_{pro}$*:GFP* fluorescence in the wild type (Col-0) and *brm-3*. Data shown are means ± SD (n = 25). Asterisks denote Student's t test significant difference between wild-type and mutant plants ($P \leq 0.05$).
(C) and **(D)** $PIN1_{pro}$*:PIN1:GFP* and $PIN2_{pro}$*:PIN2:GFP* expression in the wild type (Col-0) and *brm-3* at 3 DAG. Bars = 50 μm
(E) Quantification of $PIN1_{pro}$*:PIN1:GFP* and $PIN2_{pro}$*:PIN2:GFP* fluorescence in the wild type (Col-0) and *brm-3*. Data shown are means ± SD. Asterisks denote Student's t test significant difference between wild-type and mutant plants ($P < 0.05$).
(F) Real-time RT-PCR analysis of the expression of *PIN* genes in wild-type (Col-0), *brm-3*, and *brm-5* roots. The total RNAs were isolated from roots of the wild type (Col-0), *brm-3*, and *brm-5* (3 DAG), and *UBQ10* was used as a control. Data are means ± SD of three biological repeats. Asterisks indicate significant differences compared with wild type ($P < 0$ .05; Student's t test).

used in chromatin immunoprecipitation (ChIP) assays. Roots of 3 DAG seedlings were selected to investigate the enrichment of BRM in the different regions of the *PINs* and *PLTs* in the BRM_{pro}*:BRM:GFP* plants. ChIP-qPCR was used to determine the regions enriched by ChIP with an anti-GFP antibody, and the length of the amplicon is shown in Supplemental Table 2. As shown in Figure 6, BRM bound to the promoter and the fourth to fifth exon regions of *PIN1* (Figure 6B) as well as the promoter, transcriptional start region, and 5′-untranslated region (UTR) of *PIN2* (Figure 6C). Similarly, BRM also bound to *PIN3*, *PIN4*, and *PIN7* (Supplemental Figure 8A). These data suggest that these genes are the direct target genes regulated by BRM. In contrast, BRM did not bind to *PLT1* and *PLT2* (Supplemental Figure 9).

Previous data showed that BRM interacts with LEAFY and SEPALLATA3 proteins to alter floral organ identity by acting antagonistically with Polycomb repressors (Wu et al., 2012). BRM also antagonizes the function of Polycomb group (PcG) proteins during plant development (Li et al., 2015). PcG proteins are involved in the establishment and maintenance of the repressed chromatin state, by introducing the H3K27me3 mark. Increased levels of H3K27me3 in the *brm-3* roots were observed in the promoter, the first exon, and the fourth to fifth exon regions of *PIN1* (Figure 6D). Furthermore, increased levels of H3K27me3 in the *brm-3* roots were also observed in the promoter, the transcriptional start region, the third exon, and the 5′-UTR of *PIN2* (Figure 6E), supporting that BRM antagonizes PcG function in regulation of *PIN1* and *PIN2*. In contrast, levels of H3K27me3 in the *brm-3* roots were not changed in *PIN3*, *PIN4*, and *PIN7* (Supplemental Figure 8B). Previous studies indicated that *PIN3*, *PIN4*, and *PIN7* are not associated with H3K27me3 in 10- to 14-d-old seedlings (Zhang et al., 2007). Similarly, we also found that the levels of H3K27me3 in *PIN3*, *PIN4*, and *PIN7* were very low in both wild-type and *brm-3* roots (Supplemental Figure 8B).

DISCUSSION

BRM Acts in the PLT Pathway to Regulate Root Stem Cell Niche Maintenance

BRM, the putative enzymatic motor subunit of the SWI/SNF chromatin-remodeling complex in plants, plays an essential role in cell patterning and differentiation (Farrona et al., 2004). In this study, we demonstrated that BRM regulates stem cell niche maintenance during root development in Arabidopsis. *BRM* mutations led to markedly reduced growth of the primary roots as well as smaller meristem sizes, indicating that *BRM* is involved in root development (Figures 1A to 1C). The cellular organization of the QC and surrounding stem cells was also disrupted in *brm-1* root tips (Figures 2A and 2B). Although the QC acts as an organizer of root meristematic cells (Dolan et al., 1993; van den Berg et al., 1997; Aida et al., 2004), a low proliferation rate is observed, indicating that it can be a source for new stem cells (Dolan et al., 1993; van den Berg et al., 1995). Therefore, the fate of stem cells surrounding the QC can be used as a readout of the QC's organizing activity. By measuring the

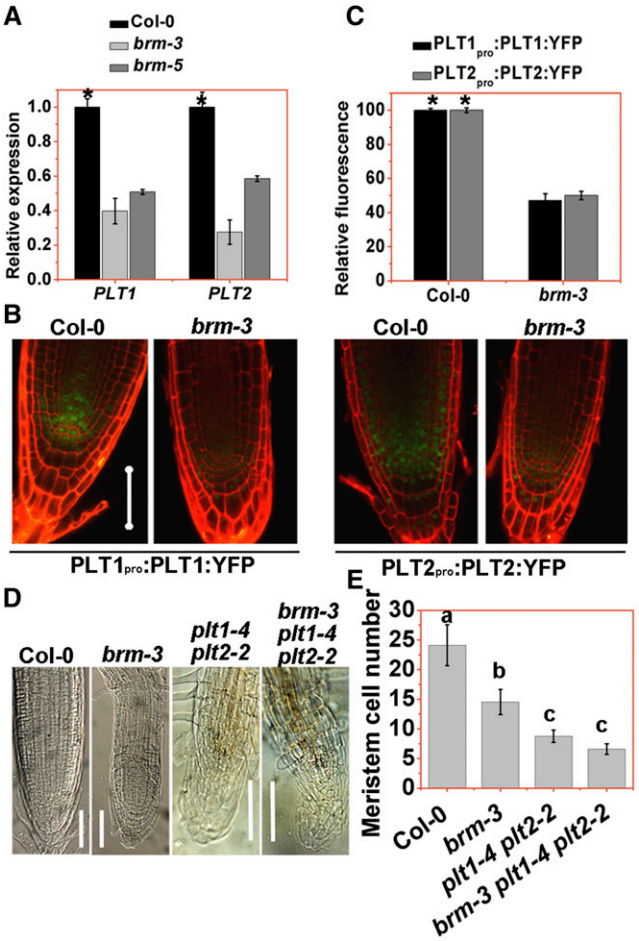

Figure 4. Mutations of *BRM* Affect the Expression of *PLT1* and *PLT2*.

(A) Real-time RT-PCR analysis of the expression of *PLT1* and *PLT2* in wild-type (Col-0), *brm-3*, and *brm-5* roots. Total RNAs were isolated from 3 DAG roots of the wild type (Col-0), *brm-3*, and *brm-5*, and *UBQ10* was used as a control. Data presented are means ± SD of three biological repeats. Asterisks indicate significant differences compared with the wild type ($P < 0.05$; Student's *t* test).

(B) *PLT1:YFP* and *PLT2:YFP* expression in wild-type (Col-0) and *brm-3* root tips at 3 DAG. Bars = 50 μm.

(C) Quantification of *PLT1:YFP* and *PLT2:YFP* fluorescence in the wild type (Col-0) and *brm-3*. Data shown are means ± SD ($n = 20$). Asterisks denote Student's *t* test significant difference between wild-type and mutant plants ($P < 0.05$).

(D) Root tips of the wild type (Col-0), *brm-3*, *plt1-4 plt2-2*, and *brm-3 plt1-4 plt2-2* single, double, and triple mutants at 3 DAG. Bars = 50 μm.

(E) Statistics of meristem cell number of the indicated genotypes at 3 DAG. Data shown are means ± SD ($n = 20$). Different letters are used to indicate means that are significantly different ($P < 0.05$, Student's *t* test).

expression of QC-specific markers and the differentiation of stem cells, we found the requirement for BRM in the maintenance of root stem cell niche. The aberrant expression of QC-specific markers such as *QC25*, *QC46*, and *QC184* indicates that BRM is essential for maintaining proper identity and activity of the QC (Figure 2C, Table 1).

In Arabidopsis roots, two main pathways specify and maintain the identity and function of QC and the associated stem cells: the SHR/SCR pathway and the auxin/PLT pathway. The SHR/SCR pathway provides positional signal along the radial axis, whereas the PLT pathway provides the longitudinal signal (Scheres, 2007; Benjamins and Scheres, 2008; Petricka and Benfey, 2008). Our study suggests that BRM acts in the auxin/PLT pathway (Supplemental Figures 5 and 6). The *BRM* mutation leads to alteration in auxin contents (Figures 3A and 3B) and local expression levels of several *PIN* genes (Figures 3C to 3F; Supplemental Figure 4). In addition, the *BRM* mutation significantly impairs *PLT1/2* expression at both the transcriptional and protein levels (Figures 4A to 4C), indicating that *BRM* plays an important role in mediating auxin-induced expression of *PLT1/2*. Furthermore, the *brm-3 plt1-1 plt2-2* and *brm-1 plt1-1 plt2-2* triple mutants have similar phenotypes to the *plt1-1 plt2-2* double mutants, supporting that BRM acts in the PLT1/2 pathway (Figures 4D and 4E; Supplemental Figure 6). Overexpression of *PLT2* can partially bypass the root meristem defects of *brm-3* (Figure 5). Taken together, these observations demonstrated that BRM regulates PLT-mediated root stem cell niche maintenance.

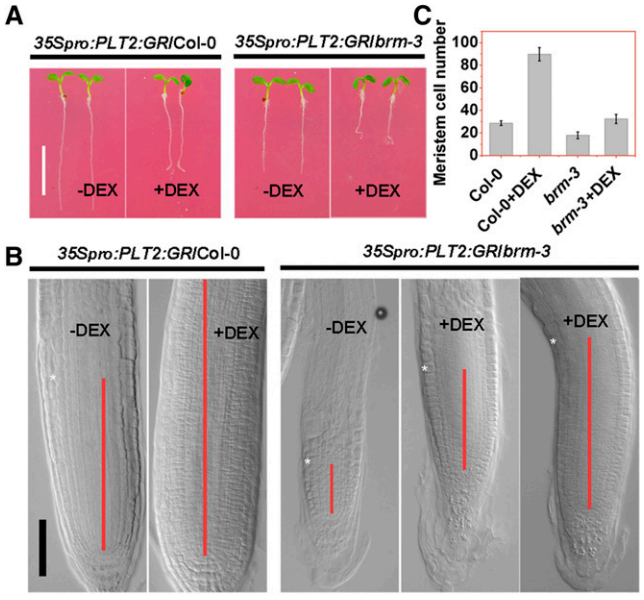

Figure 5. Overexpression of *PLT2* Partially Rescues the Root Meristem Defects of *brm-3*.

(A) Phenotypes of 5 DAG $35S_{pro}$*:PLT2:GR*/wild type (Col-0) and $35S_{pro}$*:PLT2:GR/brm-3* seedlings without or with 2 μM DEX (+DEX) treatment for 2 d. Bar = 0.5 cm.

(B) The root tips of 5 DAG $35S_{pro}$*:PLT2:GR*/Col-0 and $35S_{pro}$*:PLT2:GR/brm-3* seedlings without or with 2 μM DEX (+DEX) treatment for 2 d. Pink bars represent the root meristem of different plants extending from the QC to the transition zone. The white asterisks marked the meristem boundary where cortical cells rapidly expand. Bars = 50 μm.

(C) Quantification of the number of cortical cells in the meristem at 5 DAG, induced by $35S_{pro}$*:PLT2:GR* in the wild type (Col-0) and *brm-3* 2 d after 2 μM DEX treatment at 3 DAG. Data shown are average and SD ($n = 20$).

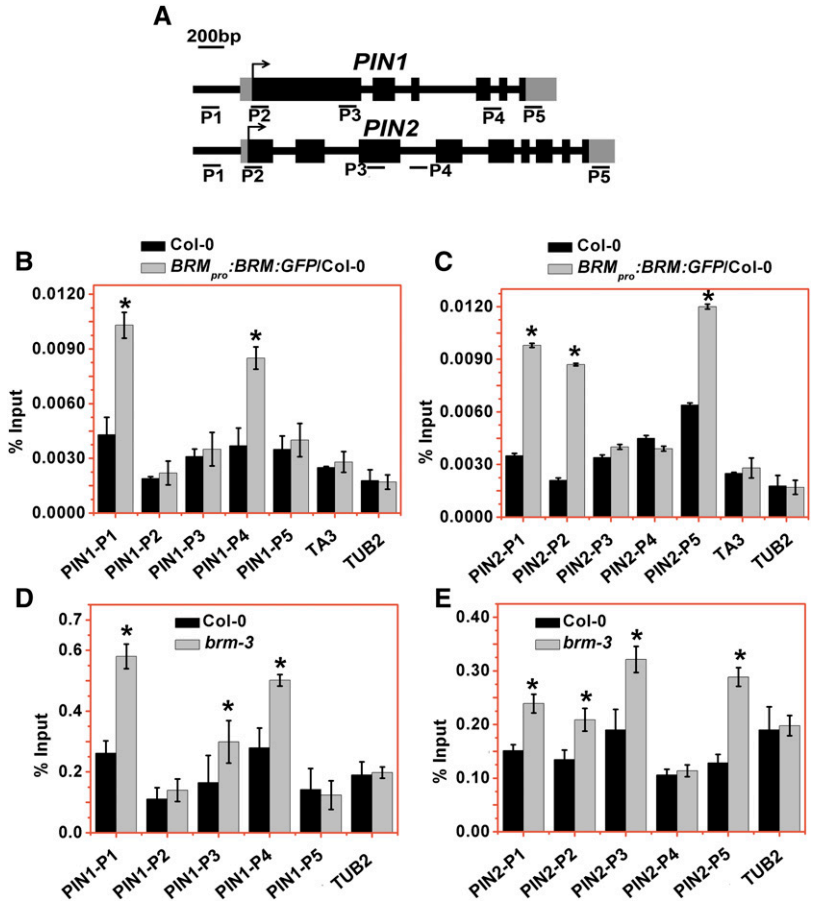

Figure 6. Binding of BRM to *PIN1* and *PIN2* Loci and the Prevalent H3K27Me3 Levels in *brm-3* Roots.

(A) Schematic diagram of *PIN1* and *PIN2*. Black boxes, gray boxes, and black lines indicate the exon, UTR, and promoter and intron of indicated genes, respectively. The regions analyzed by ChIP-qPCR are indicated by P1-P5, and the length of amplicon is shown in Supplemental Table 2.

(B) and **(C)** ChIP-qPCR analysis of enrichment of BRM_{pro}:*BRM:GFP* to the different regions of *PIN1* **(B)** and *PIN2* **(C)** in Col-0 and BRM_{pro}:*BRM:GFP*/Col-0 roots. An anti-GFP antibody was used for the immunoprecipitation. BRM_{pro}:*BRM:GFP*/Col-0 is a transgenic line expressing GFP-tagged *BRM* under the control of the *BRM* native promoter. *TA3* and *TUB2* were used as negative controls. Data are mean values ± SD of three replicates. Similar results were obtained for at least two additional independent experiments. Asterisks denote Student's *t* test significant difference between Col-0 and BRM_{pro}:*BRM:GFP*/Col-0 roots ($P < 0.05$).

(D) and **(E)** ChIP-qPCR analysis of H3K27me3 levels at the regions of *PIN1* **(D)** and *PIN2* **(E)** in Col-0 and *brm-3* mutant roots. *TUB2* was used as negative control. Data are mean values ± SD of three replicates. Similar results were obtained for at least two additional independent experiments. Asterisks denote Student's *t* test significant difference between Col-0 and *brm-3* roots.

PINs Are the Direct Target Genes Regulated by BRM

Auxins are involved in a wide range of developmental responses in plants. Graded concentrations of auxins established and maintained by auxin transport proteins are essential for embryonic, root, and shoot organogenesis (Friml et al., 2002; Benková et al., 2003; Reinhardt et al., 2003). The gradient of auxin along the roots is due to the collective activities and topology of the PIN proteins, the AUX1/LAX family proteins (Blilou et al., 2005; Grieneisen et al., 2007; Ugartechea-Chirino et al., 2010), and the multidrug-resistant/P-glycoprotein family proteins (Blakeslee et al., 2007). Auxin regulates the maintenance of the QC and the activity of the root meristem through PLTs (Galinha et al., 2007). Expression of *PLTs* is induced by PIN-driven auxin gradients; conversely, *PIN* transcription is maintained by PLT proteins to stabilize the position of the stem cell niche (Blilou et al., 2005; Grieneisen et al., 2007). Our data show that the expression of *PINs* and *PLTs* is reduced in *brm* mutant roots (Figures 3C to 3F and 4A to 4C). ChIP analysis showed that BRM bound to different regions of *PIN1*, *PIN2*, *PIN3*, *PIN4*, and *PIN7* chromatin (Figures 6B and 6C; Supplemental Figure 8A). Since no DNA binding domain was found in BRM protein, BRM may bind to *PINs* by interacting with transcription factors and other DNA binding proteins. By using yeast two-hybrid screening assays, it was demonstrated that BRM could interact with a number of transcription factors (Wu et al., 2012). More recently, it was demonstrated that BRM interacts with BP to regulate the expression of *KNAT2* and *KNAT6* in control of inflorescence

architecture (Zhao et al., 2015). Further research is required to investigate the molecular mechanism how BRM is targeted to other genomic loci such as *PINs.*

BRM Acts Antagonistically with PcG in the Regulation of *PIN1* and *PIN2*

ATP-dependent chromatin-remodeling complexes control DNA accessibility by positioning, moving, or exchanging nucleosomes via ATP-dependent alterations in histone-DNA contacts (Jiang and Pugh, 2009; Hargreaves and Crabtree, 2011). Based on the sequence similarity of their conserved ATPase subunits, they are classified into four distinct families: ISWI (ISW1a, ISW1b, and ISW2), INO80/SWR1, CHD, and SWI/SNF (including RSC) (Hota and Bartholomew, 2011). In yeast, SWI/SNF binds almost exclusively to promoters and activates its direct targets concomitant with nucleosome displacement. However, human BAF complexes are most often found in intergenic regions where they both activate and repress genes (Hargreaves and Crabtree, 2011). Similarly, the plant BRM also plays a dual role in gene transcription, since 1090 genes were downregulated, while 1115 genes were upregulated in *brm-1* mutants (Archacki et al., 2013). In yeast, the SWI/SNF complex was considered as a general activator of transcription, working in coordination with sequence-specific transactivators and the histone acetyltransferase GCN5 (Biggar and Crabtree, 1999). Indeed, stable promoter occupancy by the SWI/SNF complex requires the acetylation of the chromatin template by the histone acetyltransferase and the acetylated-lysine binding activity of the bromodomain of SWI2/SNF2 is required in this process (Hassan et al., 2002; Yamada et al., 2004; Ogiwara et al., 2011; Watanabe et al., 2013). These data indicate that histones around some loci are hyperacetylated by histone acetyltransferases, and acetylated histones are preferential targets of ATP-dependent chromatin remodeling proteins. Similar to our results, the plant histone acetyltransferases GCN5 and ADA2b regulate the expression of *PLTs* to modulate root development (Kornet and Scheres, 2009), indicating that the Arabidopsis SWI/SNF complex containing BRM may act collaboratively with histone acetyltransferases in regulating gene expression in root development.

In Drosophila, BRM was initially classified as a Trithorax group (TrxG) protein since it activates the transcription of homeotic genes and thus antagonizes the function of PcG during fly development (Tamkun et al., 1992; Hargreaves and Crabtree, 2011). Recent studies in plants indicated that SWI2/SNF2 ATPases SYD and BRM counteract PcG function in gene expression (Wu et al., 2012). These data indicate that the PcG-TrxG antagonistic regulation of gene expression is conserved between plants and metazoans, although the structures of these genes are not conserved. Nevertheless, SWI/SNF complexes also appear to cooperate together with Polycomb complexes to repress transcription at some loci (Farrona et al., 2011; Li et al., 2015). Our results show that the H3K27me3 levels of BRM binding regions were increased in *PIN1* and *PIN2* loci (Figure 6), supporting that BRM acts antagonistically with PcG functions in regulating gene expression during root development. However, the H3K27me3 levels of *PIN3*, *PIN4*, and *PIN7* loci were not changed in *brm-3* mutants (Supplemental Figure 8B), suggesting that H3K27me3 is not associated with increased *PIN3*, *PIN4*, and *PIN7* expression in the mutant. Further research is required to investigate the molecular mechanism of BRM and PcG interaction in gene regulation.

METHODS

Plant Materials and Growth Conditions

The following marker lines and mutants were used: *brm-1* (SALK_030046), *brm-3* (SALK_088462), and *brm-5* (Hurtado et al., 2006; Farrona et al., 2007; Tang et al., 2008); *QC25*, *QC46*, and *QC18* (Sabatini et al., 2003); SHR_{pro}*:GFP* (Helariutta et al., 2000); SCR_{pro}*:GFP* (Wysocka-Diller et al., 2000); $PLT1_{pro}$*:PLT1:YFP* and $PLT2_{pro}$*:PLT2:YFP* (Galinha et al., 2007); $DR5_{pro}$*:GFP* (Benková et al., 2003); $PIN1_{pro}$*:PIN1:GFP* (Benková et al., 2003); $PIN2_{pro}$*:PIN2:GFP* (Blilou et al., 2005); *shr-1* (Benfey et al., 1993); *scr-1* (Di Laurenzio et al., 1996); and *plt1-4 plt2-2* (Aida et al., 2004).

Seeds were surface-sterilized for 2 min in 75% ethanol, followed by 5 min in 1% NaClO solution and rinsed five times with sterile water, plated on Murashige and Skoog (MS) medium with 1.5% sucrose and 0.8% agar, and then stratified at 4°C in the dark for 2 d. Plants were growth under long-day conditions (16 h light/8 h dark) at 22°C in a Phytotron.

Root Meristem Size Analysis

Seeds were germinated and grown on vertically oriented plates from 1 to 14 d. Roots were examined at different days after germination depending on the experiment. Approximately 30 to 50 seedlings were examined in at least three independent experiments. Roots were mounted in chloral hydrate and then root meristem sizes were determined by counting the number of cortex cells in a file extending from the QC to the first elongated cell (Perilli and Sabatini, 2010).

Histology and Microscopy

Roots were cleared in HCG solution (chloroacetaldehyde:water:glycerol = 8:3:1) for several minutes before microscopy analysis. For Lugol staining, roots were incubated in Lugol solution (Sigma-Aldrich) for 3 to 5 s, then washed by water and mounted in HCG solution for microscopy. Histochemical staining for GUS activity in homozygous transgenic plants was performed according to the described method (Jefferson et al., 1987). Whole seedlings were immersed in the GUS staining solution (1 mM X-glucuronide in 100 mM sodium phosphate, pH 7.2, 0.5 mM ferricyanide, 0.5 mM ferrocyanide, and 0.1% Triton X-100) and incubated at 37°C in the dark from 2 to 8 h depending on the experimental requirement. To determine the expression pattern of QC markers, we measured the GUS staining area using Digimizer image analysis software (http://www.digimizer.com). The staining areas between 50 and 90 μm^2 were defined as "normal expression," those lower than 50 μm^2 as "reduced expression," and those bigger than 90 μm^2 as "expanded expression." Plants on MS medium were photographed using the Leica DFC 490 stereomicroscope and Leica DM5000B microscope. Images were processed with Adobe Photoshop CS 8.0 software.

Homozygous transgenic plants were used for confocal imaging. Cell walls were labeled with propidium iodide (PI) as described (Truernit and Haseloff, 2008). Roots were counterstained with 10 $\mu g\ mL^{-1}$ PI (Sigma-Aldrich) for 5 min, washed once in distilled water, and mounted in water for confocal microscopy. Confocal images were taken using a Zeiss LSM 710 laser scanning microscope with the following excitation (Ex) and emission (Em) wavelengths (Ex/Em): 561 nm/591 to 635 nm for PI, 488 nm/505 to 530 nm for GFP, and 514 nm/530 to 600 nm for YFP. The objective lenses 20× and 40× were used. Fluorescence was quantified with the LAS AF Lite program on confocal sections acquired with the same microscope settings. Approximately 10 to 15 images were examined, and at least two

independent experiments were performed. The statistical significance was evaluated by Student's *t* test analysis.

Gene Expression Analyses

Total RNA from 3 DAG roots was extracted with Trizol reagent (Invitrogen) according to the manufacturer's protocol and used to synthesize cDNA. The gene-specific primers used for real-time PCR are listed in Supplemental Table 1. Each sample was quantified at least in triplicate and normalized using *Ubiquitin10* (*UBQ10*) as an internal control.

ChIP Assays

Roots (~0.3 g) from 3 DAG seedlings grown on vertically oriented plates with MS medium were collected for ChIP assays (Gendrel et al., 2005; Liu et al., 2012). After fixation with formaldehyde, the chromatin was sheared to an average length of 500 bp by sonication and then immunoprecipitated with GFP-Trap_A agarose beads (ChromoTek) or H3K27me3 antibody (Millipore 07-449). After cross-linking was reversed, the amount of precipitated DNA fragments and input DNA was detected by quantitative real-time PCR using specific primers listed in Supplemental Table 2. The percentage of input was calculated by determining $2^{-\Delta Ct}$ ($=2^{-[Ct(ChIP)-Ct(Input)]}$). The exon region of retrotransposon *TA3* (Han et al., 2012) and *TUB2* was used as negative control.

Accession Numbers

Sequence data from this article can be found in the Arabidopsis Genome initiative or GenBank/EMBL databases under the following accession numbers: *BRM* (*AT2G46020*), *SCR* (*AT3G54220*), *SHR* (*AT4G37650*), *PLT1* (*AT3G20840*), *PLT2* (*AT1G51190*), *PIN1* (*AT1G73590*), *PIN2* (*AT5G57090*), *PIN3* (*AT1G70940*), *PIN4* (*AT2G01420*), *PIN7* (*AT1G23080*), *CycB1;1* (*AT4G37490*), and *CycB1;3* (*AT3G11520*).

Supplemental Data

Supplemental Figure 1. The lateral root number in wild-type, *brm-1*, *brm-3*, and *brm-5* roots 10 DAG.

Supplemental Figure 2. The expression of *CycB1;1* and *CycB1;3* in 3 DAG wild-type, *brm-3*, and *brm-5* roots.

Supplemental Figure 3. Cellular organization of wild-type (Col-0), *brm-3*, *brm-5*, and *brm-1* root tips at 3 DAG.

Supplemental Figure 4. The expression of *PIN2* in wild-type (Col-0) and *brm-3* root tips at 3 DAG and the expression of root development related genes in wild-type (Col-0) and *brm-1* 5-d-old seedlings.

Supplemental Figure 5. The expression pattern of SHR and SCR in the wild type and *brm-3* and the phenotype of *shr-1 brm-3*, *scr-1 brm-3*, *shr-1 brm-1*, and *scr-1 brm-1* double mutants.

Supplemental Figure 6. The phenotype of *brm-1 plt1-4 plt2-2* and *brm-3 plt1-4 plt2-2* triple mutants at 7 DAG.

Supplemental Figure 7. The phenotype of Col-0 and BRM_{pro}*:BRM:GFP/brm-1* seedlings at 10 DAG.

Supplemental Figure 8. ChIP-qPCR analysis of BRM targeting to *PIN3*, *PIN4*, and *PIN7* and H3K27me3 levels of *PIN3*, *PIN4*, and *PIN7* loci in *brm-3* mutant roots.

Supplemental Figure 9. BRM does not target to *PLT1* and *PLT2* directly.

Supplemental Figure 10. The normal expression of QC25 and QC46 in wild-type (Col-0) and *brm-3* root tips at 3 DAG.

Supplemental Table 1. Primers used for RT-qPCR.

Supplemental Table 2. Primers used for ChIP-qPCR.

ACKNOWLEDGMENTS

We thank Philip Benfey (Duke University) for providing *35Spro:PLT2:GR* seeds, Ben Scheres (Utrecht University) for *shr-1* and *scr-1* seeds, Lizhen Tao (South China Agricultural University) for *plt1-1/plt2-1* seeds, and the ABRC for kindly providing seeds used in this study. This work was supported by grants from the National Basic Research Program of China (973 Program No. 2012CB910900), the National Natural Science Foundation of China (No. 31201106 and No. 31371308), and the Ministry of Science and Technology of Taiwan (101-2311-B-002-012-MY3 and 103-2321-B-002-039).

AUTHOR CONTRIBUTIONS

S.Y. and K.W. conceived this project and designed all research. S.Y., C.L., L.Z., S.G., J.L., M.Z., C.-Y.C., X.L., and M.L. performed the research. S.Y., Y.C., C.L., C.Y., and K.W. analyzed data. S.Y. and K.W. wrote the article.

Received January 30, 2015; revised April 24, 2015; accepted May 5, 2015; published May 19, 2015.

REFERENCES

Aida, M., Beis, D., Heidstra, R., Willemsen, V., Blilou, I., Galinha, C., Nussaume, L., Noh, Y.S., Amasino, R., and Scheres, B. (2004). The PLETHORA genes mediate patterning of the *Arabidopsis* root stem cell niche. Cell **119:** 109–120.

Archacki, R., et al. (2013). BRAHMA ATPase of the SWI/SNF chromatin remodeling complex acts as a positive regulator of gibberellin-mediated responses in *Arabidopsis.* PLoS ONE **8:** e58588.

Benfey, P.N., Linstead, P.J., Roberts, K., Schiefelbein, J.W., Hauser, M.T., and Aeschbacher, R.A. (1993). Root development in *Arabidopsis*: four mutants with dramatically altered root morphogenesis. Development **119:** 57–70.

Benjamins, R., and Scheres, B. (2008). Auxin: the looping star in plant development. Annu. Rev. Plant Biol. **59:** 443–465.

Benková, E., Michniewicz, M., Sauer, M., Teichmann, T., Seifertová, D., Jürgens, G., and Friml, J. (2003). Local, efflux-dependent auxin gradients as a common module for plant organ formation. Cell **115:** 591–602.

Biggar, S.R., and Crabtree, G.R. (1999). Continuous and widespread roles for the Swi-Snf complex in transcription. EMBO J. **18:** 2254–2264.

Blakeslee, J.J., et al. (2007). Interactions among PIN-FORMED and P-glycoprotein auxin transporters in *Arabidopsis.* Plant Cell **19:** 131–147.

Blilou, I., Xu, J., Wildwater, M., Willemsen, V., Paponov, I., Friml, J., Heidstra, R., Aida, M., Palme, K., and Scheres, B. (2005). The PIN auxin efflux facilitator network controls growth and patterning in *Arabidopsis* roots. Nature **433:** 39–44.

Cairns, B.R. (2005). Chromatin remodeling complexes: strength in diversity, precision through specialization. Curr. Opin. Genet. Dev. **15:** 185–190.

Cairns, B.R., Kim, Y.J., Sayre, M.H., Laurent, B.C., and Kornberg, R.D. (1994). A multisubunit complex containing the SWI1/ADR6, SWI2/SNF2, SWI3, SNF5, and SNF6 gene products isolated from yeast. Proc. Natl. Acad. Sci. USA **91:** 1950–1954.

Colón-Carmona, A., You, R., Haimovitch-Gal, T., and Doerner, P. (1999). Technical advance: spatio-temporal analysis of mitotic activity with a labile cyclin-GUS fusion protein. Plant J. **20:** 503–508.

Côté, J., Quinn, J., Workman, J.L., and Peterson, C.L. (1994). Stimulation of GAL4 derivative binding to nucleosomal DNA by the yeast SWI/SNF complex. Science **265:** 53–60.

Cui, H., Levesque, M.P., Vernoux, T., Jung, J.W., Paquette, A.J., Gallagher, K.L., Wang, J.Y., Blilou, I., Scheres, B., and Benfey, P.N. (2007). An evolutionarily conserved mechanism delimiting SHR movement defines a single layer of endodermis in plants. Science **316:** 421–425.

Di Laurenzio, L., Wysocka-Diller, J., Malamy, J.E., Pysh, L., Helariutta, Y., Freshour, G., Hahn, M.G., Feldmann, K.A., and Benfey, P.N. (1996). The *SCARECROW* gene regulates an asymmetric cell division that is essential for generating the radial organization of the Arabidopsis root. Cell **86:** 423–433.

Dinneny, J.R., and Benfey, P.N. (2008). Plant stem cell niches: standing the test of time. Cell **132:** 553–557.

Dolan, L., Janmaat, K., Willemsen, V., Linstead, P., Poethig, S., Roberts, K., and Scheres, B. (1993). Cellular organisation of the *Arabidopsis thaliana* root. Development **119:** 71–84.

Efroni, I., Han, S.K., Kim, H.J., Wu, M.F., Steiner, E., Birnbaum, K. D., Hong, J.C., Eshed, Y., and Wagner, D. (2013). Regulation of leaf maturation by chromatin-mediated modulation of cytokinin responses. Dev. Cell **24:** 438–445.

Farrona, S., Hurtado, L., and Reyes, J.C. (2007). A nucleosome interaction module is required for normal function of *Arabidopsis thaliana* BRAHMA. J. Mol. Biol. **373:** 240–250.

Farrona, S., Hurtado, L., Bowman, J.L., and Reyes, J.C. (2004). The *Arabidopsis thaliana* SNF2 homolog AtBRM controls shoot development and flowering. Development **131:** 4965–4975.

Farrona, S., Hurtado, L., March-Díaz, R., Schmitz, R.J., Florencio, F.J., Turck, F., Amasino, R.M., and Reyes, J.C. (2011). Brahma is required for proper expression of the floral repressor *FLC* in *Arabidopsis.* PLoS ONE **6:** e17997.

Friml, J., Vieten, A., Sauer, M., Weijers, D., Schwarz, H., Hamann, T., Offringa, R., and Jürgens, G. (2003). Efflux-dependent auxin gradients establish the apical-basal axis of *Arabidopsis.* Nature **426:** 147–153.

Friml, J., Benková, E., Blilou, I., Wisniewska, J., Hamann, T., Ljung, K., Woody, S., Sandberg, G., Scheres, B., Jürgens, G., and Palme, K. (2002). AtPIN4 mediates sink-driven auxin gradients and root patterning in *Arabidopsis.* Cell **108:** 661–673.

Galinha, C., Hofhuis, H., Luijten, M., Willemsen, V., Blilou, I., Heidstra, R., and Scheres, B. (2007). PLETHORA proteins as dose-dependent master regulators of *Arabidopsis* root development. Nature **449:** 1053–1057.

Gendrel, A.V., Lippman, Z., Martienssen, R., and Colot, V. (2005). Profiling histone modification patterns in plants using genomic tiling microarrays. Nat. Methods **2:** 213–218.

Grieneisen, V.A., Xu, J., Marée, A.F.M., Hogeweg, P., and Scheres, B. (2007). Auxin transport is sufficient to generate a maximum and gradient guiding root growth. Nature **449:** 1008–1013.

Han, S.K., Sang, Y., Rodrigues, A., Wu, M.F., Rodriguez, P.L., and Wagner, D., BIOL425 F2010 (2012). The SWI2/SNF2 chromatin remodeling ATPase BRAHMA represses abscisic acid responses in the absence of the stress stimulus in *Arabidopsis.* Plant Cell **24:** 4892–4906.

Hargreaves, D.C., and Crabtree, G.R. (2011). ATP-dependent chromatin remodeling: genetics, genomics and mechanisms. Cell Res. **21:** 396–420.

Hassan, A.H., Prochasson, P., Neely, K.E., Galasinski, S.C., Chandy, M., Carrozza, M.J., and Workman, J.L. (2002). Function and selectivity of bromodomains in anchoring chromatin-modifying complexes to promoter nucleosomes. Cell **111:** 369–379.

Helariutta, Y., Fukaki, H., Wysocka-Diller, J., Nakajima, K., Jung, J., Sena, G., Hauser, M.T., and Benfey, P.N. (2000). The *SHORT-ROOT* gene controls radial patterning of the *Arabidopsis* root through radial signaling. Cell **101:** 555–567.

Hota, S.K., and Bartholomew, B. (2011). Diversity of operation in ATP-dependent chromatin remodelers. Biochim. Biophys. Acta **1809:** 476–487.

Hurtado, L., Farrona, S., and Reyes, J.C. (2006). The putative SWI/SNF complex subunit BRAHMA activates flower homeotic genes in *Arabidopsis thaliana.* Plant Mol. Biol. **62:** 291–304.

Jefferson, R.A., Kavanagh, T.A., and Bevan, M.W. (1987). GUS fusions: beta-glucuronidase as a sensitive and versatile gene fusion marker in higher plants. EMBO J. **6:** 3901–3907.

Jerzmanowski, A. (2007). SWI/SNF chromatin remodeling and linker histones in plants. Biochim. Biophys. Acta **1769:** 330–345.

Jiang, C., and Pugh, B.F. (2009). Nucleosome positioning and gene regulation: advances through genomics. Nat. Rev. Genet. **10:** 161–172.

Knizewski, L., Ginalski, K., and Jerzmanowski, A. (2008). Snf2 proteins in plants: gene silencing and beyond. Trends Plant Sci. **13:** 557–565.

Koizumi, K., and Gallagher, K.L. (2013). Identification of SHRUBBY, a SHORT-ROOT and SCARECROW interacting protein that controls root growth and radial patterning. Development **140:** 1292–1300.

Kornet, N., and Scheres, B. (2009). Members of the GCN5 histone acetyltransferase complex regulate PLETHORA-mediated root stem cell niche maintenance and transit amplifying cell proliferation in *Arabidopsis.* Plant Cell **21:** 1070–1079.

Kwon, C.S., Hibara, K., Pfluger, J., Bezhani, S., Metha, H., Aida, M., Tasaka, M., and Wagner, D. (2006). A role for chromatin remodeling in regulation of *CUC* gene expression in the *Arabidopsis* cotyledon boundary. Development **133:** 3223–3230.

Levesque, M.P., Vernoux, T., Busch, W., Cui, H., Wang, J.Y., Blilou, I., Hassan, H., Nakajima, K., Matsumoto, N., Lohmann, J.U., Scheres, B., and Benfey, P.N. (2006). Whole-genome analysis of the SHORT-ROOT developmental pathway in *Arabidopsis.* PLoS Biol. **4:** e143.

Li, C., Chen, C., Gao, L., Yang, S., Nguyen, V., Shi, X., Siminovitch, K., Kohalmi, S.E., Huang, S., Wu, K., Chen, X., and Cui, Y. (2015). The *Arabidopsis* SWI2/SNF2 chromatin Remodeler BRAHMA regulates polycomb function during vegetative development and directly activates the flowering repressor gene *SVP.* PLoS Genet. **11:** e1004944.

Liu, X., Yu, C.W., Duan, J., Luo, M., Wang, K., Tian, G., Cui, Y., and Wu, K. (2012). HDA6 directly interacts with DNA methyltransferase MET1 and maintains transposable element silencing in *Arabidopsis.* Plant Physiol. **158:** 119–129.

Mähönen, A.P., ten Tusscher, K., Siligato, R., Smetana, O., Díaz-Triviño, S., Salojärvi, J., Wachsman, G., Prasad, K., Heidstra, R., and Scheres, B. (2014). PLETHORA gradient formation mechanism separates auxin responses. Nature **515:** 125–129.

Nakajima, K., Sena, G., Nawy, T., and Benfey, P.N. (2001). Intercellular movement of the putative transcription factor SHR in root patterning. Nature **413:** 307–311.

Neigeborn, L., and Carlson, M. (1984). Genes affecting the regulation of SUC2 gene expression by glucose repression in *Saccharomyces cerevisiae.* Genetics **108:** 845–858.

Ogiwara, H., Ui, A., Otsuka, A., Satoh, H., Yokomi, I., Nakajima, S., Yasui, A., Yokota, J., and Kohno, T. (2011). Histone acetylation by CBP and p300 at double-strand break sites facilitates SWI/SNF chromatin remodeling and the recruitment of non-homologous end joining factors. Oncogene **30:** 2135–2146.

Ohkawa, Y., Marfella, C.G.A., and Imbalzano, A.N. (2006). Skeletal muscle specification by myogenin and Mef2D via the SWI/SNF ATPase Brg1. EMBO J. **25:** 490–501.

Pedersen, T.A., Kowenz-Leutz, E., Leutz, A., and Nerlov, C. (2001). Cooperation between C/EBPalpha TBP/TFIIB and SWI/SNF recruiting domains is required for adipocyte differentiation. Genes Dev. **15:** 3208–3216.

Perilli, S., and Sabatini, S. (2010). Analysis of root meristem size development. Methods Mol. Biol. **655:** 177–187.

Peterson, C.L., Dingwall, A., and Scott, M.P. (1994). Five SWI/SNF gene products are components of a large multisubunit complex

required for transcriptional enhancement. Proc. Natl. Acad. Sci. USA **91:** 2905–2908.

Petricka, J.J., and Benfey, P.N. (2008). Root layers: complex regulation of developmental patterning. Curr. Opin. Genet. Dev. **18:** 354–361.

Reinhardt, D., Pesce, E.R., Stieger, P., Mandel, T., Baltensperger, K., Bennett, M., Traas, J., Friml, J., and Kuhlemeier, C. (2003). Regulation of phyllotaxis by polar auxin transport. Nature **426:** 255–260.

Sabatini, S., Heidstra, R., Wildwater, M., and Scheres, B. (2003). SCARECROW is involved in positioning the stem cell niche in the *Arabidopsis* root meristem. Genes Dev. **17:** 354–358.

Sabatini, S., Beis, D., Wolkenfelt, H., Murfett, J., Guilfoyle, T., Malamy, J., Benfey, P., Leyser, O., Bechtold, N., Weisbeek, P., and Scheres, B. (1999). An auxin-dependent distal organizer of pattern and polarity in the *Arabidopsis* root. Cell **99:** 463–472.

Scheres, B. (2007). Stem-cell niches: nursery rhymes across kingdoms. Nat. Rev. Mol. Cell Biol. **8:** 345–354.

Smaczniak, C., et al. (2012). Characterization of MADS-domain transcription factor complexes in *Arabidopsis* flower development. Proc. Natl. Acad. Sci. USA **109:** 1560–1565.

Stern, M., Jensen, R., and Herskowitz, I. (1984). Five SWI genes are required for expression of the HO gene in yeast. J. Mol. Biol. **178:** 853–868.

Tamkun, J.W., Deuring, R., Scott, M.P., Kissinger, M., Pattatucci, A.M., Kaufman, T.C., and Kennison, J.A. (1992). brahma: a regulator of Drosophila homeotic genes structurally related to the yeast transcriptional activator SNF2/SWI2. Cell **68:** 561–572.

Tang, X., Hou, A., Babu, M., Nguyen, V., Hurtado, L., Lu, Q., Reyes, J.C., Wang, A., Keller, W.A., Harada, J.J., Tsang, E.W.T., and Cui, Y. (2008). The *Arabidopsis* BRAHMA chromatin-remodeling ATPase is involved in repression of seed maturation genes in leaves. Plant Physiol. **147:** 1143–1157.

Truernit, E., and Haseloff, J. (2008). A simple way to identify non-viable cells within living plant tissue using confocal microscopy. Plant Methods **4:** 15.

Ugartechea-Chirino, Y., Swarup, R., Swarup, K., Péret, B., Whitworth, M., Bennett, M., and Bougourd, S. (2010). The AUX1 LAX family of auxin influx carriers is required for the establishment of embryonic root cell organization in *Arabidopsis thaliana.* Ann. Bot. (Lond.) **105:** 277–289.

Ulmasov, T., Murfett, J., Hagen, G., and Guilfoyle, T.J. (1997). Aux/IAA proteins repress expression of reporter genes containing natural and highly active synthetic auxin response elements. Plant Cell **9:** 1963–1971.

van den Berg, C., Willemsen, V., Hage, W., Weisbeek, P., and Scheres, B. (1995). Cell fate in the Arabidopsis root meristem determined by directional signalling. Nature **378:** 62–65.

van den Berg, C., Willemsen, V., Hendriks, G., Weisbeek, P., and Scheres, B. (1997). Short-range control of cell differentiation in the *Arabidopsis* root meristem. Nature **390:** 287–289.

Vercruyssen, L., et al. (2014). ANGUSTIFOLIA3 binds to SWI/SNF chromatin remodeling complexes to regulate transcription during Arabidopsis leaf development. Plant Cell **26:** 210–229.

Watanabe, S., Radman-Livaja, M., Rando, O.J., and Peterson, C.L. (2013). A histone acetylation switch regulates H2A.Z deposition by the SWR-C remodeling enzyme. Science **340:** 195–199.

Wildwater, M., Campilho, A., Perez-Perez, J.M., Heidstra, R., Blilou, I., Korthout, H., Chatterjee, J., Mariconti, L., Gruissem, W., and Scheres, B. (2005). The RETINOBLASTOMA-RELATED gene regulates stem cell maintenance in *Arabidopsis* roots. Cell **123:** 1337–1349.

Wu, M.F., Sang, Y., Bezhani, S., Yamaguchi, N., Han, S.K., Li, Z., Su, Y., Slewinski, T.L., and Wagner, D. (2012). SWI2/SNF2 chromatin remodeling ATPases overcome polycomb repression and control floral organ identity with the LEAFY and SEPALLATA3 transcription factors. Proc. Natl. Acad. Sci. USA **109:** 3576–3581.

Wysocka-Diller, J.W., Helariutta, Y., Fukaki, H., Malamy, J.E., and Benfey, P.N. (2000). Molecular analysis of SCARECROW function reveals a radial patterning mechanism common to root and shoot. Development **127:** 595–603.

Yamada, T., Mizuno, K., Hirota, K., Kon, N., Wahls, W.P., Hartsuiker, E., Murofushi, H., Shibata, T., and Ohta, K. (2004). Roles of histone acetylation and chromatin remodeling factor in a meiotic recombination hotspot. EMBO J. **23:** 1792–1803.

Zhang, X., Clarenz, O., Cokus, S., Bernatavichute, Y.V., Pellegrini, M., Goodrich, J., and Jacobsen, S.E. (2007). Whole-genome analysis of histone H3 lysine 27 trimethylation in Arabidopsis. PLoS Biol. **5:** e129.

Zhao, M., Yang, S., Chen, C.Y., Li, C., Shan, W., Lu, W., Cui, Y., Liu, X., and Wu, K. (2015). Arabidopsis BREVIPEDICELLUS interacts with the SWI2/SNF2 chromatin remodeling ATPase BRAHMA to regulate *KNAT2* and *KNAT6* expression in control of inflorescence architecture. PLoS Genet. **11:** e1005125.

Zhu, Y., Rowley, M.J., Böhmdorfer, G., and Wierzbicki, A.T. (2013). A SWI/SNF chromatin-remodeling complex acts in noncoding RNA-mediated transcriptional silencing. Mol. Cell **49:** 298–309.